LIFETIME ESTIMATION OF MOVING VESICLES IN FREQUENCY-DOMAIN FLUORESCENCE LIFETIME IMAGING MICROSCOPY

Philippe Roudot, Charles Kervrann

Inria Rennes - Bretagne Atlantique
35 042 Rennes Cedex, France

François Waharte

UMR 144 CNRS - PICT IBiSA - Institut Curie
75 248 Paris V, France

ABSTRACT

We propose a robust statistical framework for correcting the movements of vesicles in frequency domain FLIM imaging. Movement and lifetime are jointly estimated in a three-step procedure. Robust M-estimators are mainly used to improve accuracy in temporally-varying noisy images. The performance of the proposed method is demonstrated on both simulated and real samples.

***Index Terms*—** FLIM, frequency-domain, phase modulation, spot tracking, template matching, M-estimation

1. INTRODUCTION

Fluorescence lifetime imaging microscopy (FLIM) is now a widely spread imaging technique for sensing fluorophore environment in a living biological sample (like pH, ions...). Fluorescence lifetime (i.e. average time of a fluorophore staying in excited state before relaxing to its ground state and possibly emitting a photon) is particularly useful to detect the Förster resonance energy transfer (FRET) which can allow to quantify spatial proximity between neighboring molecules [1]. Such *in vivo* techniques are known to be more precise than *in vitro* biochemical methods. Now the former gives a much better analysis of the global phenomenon than a sample-by-sample FLIM measure carried out by an operator. To overcome this problem, automatization of FLIM sample analysis is required.

In comparison to the well-established time-correlated single-photon counting (TCSPC) technique, frequency-domain methods are known to be faster [2]. Nevertheless, since it relies on intensity quantification over an image series, it is sensitive to sample movement that may lead to additional intensity variations [2]. To address this problem we propose a framework that exploits the intensity model of the frequency-domain FLIM output to jointly estimate trajectories and lifetimes of vesicles.

To our knowledge, no previous work have been done on this specific topic; Fourier transform or sine fitting is often recommended in the case of static molecules [3, 4]. However, a wealth of methods have already been proposed to track molecules in fluorescence imaging. Most of them rely on particle linking after spot detection in each frame [5, 6]. Spot detection can be performed using multi-scale wavelet analysis, top-hat filtering or local curvature analysis (see [7]). Other approaches are based on template cross-correlation [8]. Our tracking approach is especially inspired from Gaussian fitting techniques [9].

In this paper we propose a statistical framework that combines lifetime estimation and robust M-estimator-based tracking in a efficient and fast way. We present a three-step procedure to estimate the movement and the lifetime of vesicles : sinusoid parameters prediction (step 1), robust tracking exploiting the former prediction (step 2) and lifetime estimation (step 3). Spot detection is performed on the initial frame. Actually, we do not need sophisticated spot detection scheme since our estimator will diverge on objects which are not conform with our model. This saves computations for applications.

The remainder of this paper is organized as follows: Section 2 briefly presents the physical process related to frequency-domain FLIM measurements. In Section 3, we describe our vesicle template model and we present the procedure devoted to the estimation of movement and lifetime. Section 4 presents experimental results.

2. FLUORESCENCE LIFETIME MEASUREMENT BY HOMODYNE DETECTION

FD FLIM images have a very specific intensity footprint which needs to be described for a better understanding of our approach. This section briefly presents the theoretical basis for lifetime measurement in FD-FLIM by homodyne detection (see [4] for a more detailed description).

Given a fluorescence sample excited with a single laser pulse, the impulse response $R(t)$ can be described by a sum of exponential function parameterized by decay times: these lifetimes represent the average time between its excitation time and return time to the ground state of each molecule present in the sample. For the sake of simplicity, we assume the fluorescence decay to be described by a single exponential decay $R(t) = R_0 e^{-t^2/\tau^2}$ where R_0 is the intensity at $t = 0$

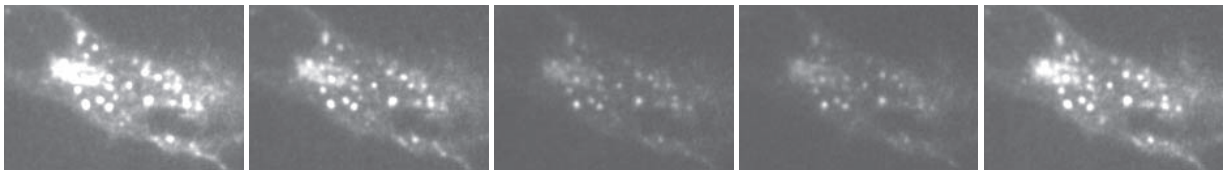


Fig. 1. An example of frequency-domain FLIM measurement with $K = 5$ modulation signals (contrasts are enhanced for visualization).

and τ is the decay time.

Whereas the excitation source in time-domain methods is a laser pulse (like with TCPSC), the FD source is a sinusoidally modulated excitation $E(t)$ defined as:

$$E(t) = C_E + A_E \sin(\omega_E t + \Phi_E) \quad (1)$$

where ω_E denotes the radial frequency of the excitation signal, C_E the offset, A_E the amplitude and Φ_E is the phase delay. Hence, the emitted fluorescent signal is defined as :

$$\begin{aligned} F(t) &= E(t) * R(t) \\ &= C_F + A_F \sin(\omega_E t + \Phi_E - \arctan(\omega_E \tau)) \end{aligned} \quad (2)$$

where $*$ denotes the convolution operator. Accordingly, the phase delay $\Phi_E - \arctan(\omega_E \tau)$ of $F(t)$ allows us to recover τ. In an experimental setup, the frequency (> 1 MHz) is too high to be compatible with CCD sensor frame rate. Therefore the signal $F(t)$ is phase-modulated with K sinusoidal signals $M_k(t), k \in [1, K]$ at frequency ω_E (homodyne detection):

$$M_k(t) = C_M + A_M \sin\left(\omega_E t + \Phi_{M_0} + \frac{2\pi k}{K}\right). \quad (3)$$

Thanks to the low pass effect of the CCD detector, the higher frequencies of the phase modulated-signal $F(t)M_k(t)$ are negligible. Therefore we obtain K time-independent signals described as a function of $k \in [1, K]$ (see Fig. 1):

$$S_\theta(k) = \mathcal{G}_{\text{ccd}}(F(t)M_k(t)) = C_S + A_S \cos\left(\frac{2\pi k}{K} + \Phi_\tau\right) \quad (4)$$

where $C_S = C_F C_M$, $A_S = A_F A_M$ and Φ_τ is the phase. In what follows, we denote $\theta = (C_S, A_S, \Phi_\tau)^T$. The phase

$$\Phi_\tau = (\Phi_{M_0} - \Phi_E + \arctan(\omega_E \tau)) \quad (5)$$

can be recovered using sine fitting or Fourier decomposition techniques from the lower frequency of $S_\theta(k)$. The phase delay $(\Phi_{M_0} - \Phi_E)$ of the system is calibrated by recording a reference frame sequence of a fluorescent sample with known lifetime. Finally, as we monitor the frequency ω_E, τ comes straightforwardly. Figure 2 shows an example of lifetime computation using the Fourier transform and specific locations highlights the problem of moving vesicles which generate unrealistic values.

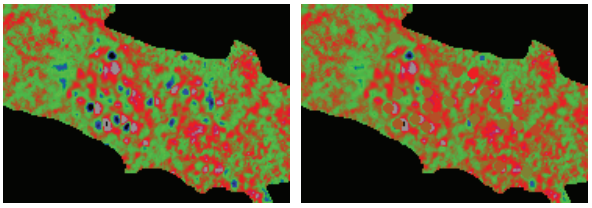


Fig. 2. Left: Lifetime map using Fourier decomposition. Blue and grey spots are unrealistic values due to organels movement. Right: improvement of the lifetime map reconstruction using our method.

3. LIFETIME ESTIMATION ON VESICLES

The method presented above has been successfully applied on immobilized samples [2]. However considering moving vesicles is crucial when studying energy transfer. This study focus especially on moving sub-resolution vesicles. In this section we propose a model to describe the spatial and temporal variations of vesicles through the stack of K frames. In the following we use time to refer to the order of phase-modulated frames. To alleviate complexity while taking into account the correlation of parameters, we propose a three-step estimation procedure where the estimation of lifetime parameter and the movement parameter are decoupled.

3.1. Modeling spatial and temporal variations

Several degradations were taken into account to model the vesicle intensity. In our approach the microscope point spread function (PSF), corresponding to a Bessel function, is approximated as a Gaussian function. Secondly, as the confocal equipment is not rigorously stigmatic the signal is composed of a background and a pinpoint vesicle before microscope diffraction. The background also follows the model (4) due to cytoplasmic fluorescence. Finally the background is assumed to be smooth over the PSF support. Let $I(k)(x)$ be the intensity on frame k at location $x \in \Omega$ (pixel grid):

$$I(k)(x) = S_{\theta_b}(k)(x) + S_{\theta_0}(k) G_\gamma(x - x_0(k)) + \varepsilon(k)(x) \quad (6)$$

where $S_{\theta_0}(k)$ is the vesicle mean intensity parameterized by $\theta_0 = (C_{S_0}, A_{S_0}, \Phi_{\tau_0})^T$ as in (4), $S_{\theta_b}(k)(x)$ is the background signal parameterized by $\theta_b(x) = (C_{S_b}(x), A_{S_b}(x), \Phi_{\tau_b}(x))^T$, $G_\gamma(x)$ is a Gaussian function of variance γ^2 centered at the

origin which describes the shape of the vesicle, $x_0(k)$ is the position of the vesicle on frame k, ε is the additive noise introduced by the system. All the parameters will be estimated in our procedure but $\theta_b(x)$ needs to be estimated only on the vicinity of a vesicle.

3.2. A three-step estimation procedure

In this section, we present the three-step parameter estimation procedure leading to a robust estimation of the intensity decay time τ_0: sinusoid parameters prediction, robust tracking exploiting this prediction, lifetime estimation.

Step 1: Sinusoid parameter prediction

First, we consider a small number of frames $K^- < K$ (typically $K^- = 3$ when $K = 12$) to predict θ_0 and we study a simpler intensity model for $k \in [1, K^-]$ by neglecting the background influence:

$$I(k)(x) = S_{\theta_0}(k)G_\gamma(x - x_0(k)) + \varepsilon(k)(x). \quad (7)$$

Vesicles are first tracked using a simple Gaussian fitting [9] over a square 7×7 window W. Before tracking, spot are detected using derivative of Gaussian filtering. Those tracks provides us with estimations $x_0^-(k)$ and γ^-. Thus we can estimate θ_0 by minimizing a robust error function:

$$\theta_0^- = \underset{\theta_0}{\operatorname{argmin}} \quad (8)$$
$$\sum_{k\in[1,K]} \sum_{x\in W(x_0^-(k))} \rho_{\eta_1}\left(I(k)(x) - S_{\theta_0}(k)G_{\gamma^-}(x - x_0^-(k))\right)$$

where $W(x_0^-(k))$ is a 7×7 window centered at $x_0^-(k)$. The function ρ is an influence function chosen with a scale parameter $\eta_1 = \lambda_1\sigma_{LTS}$ used to weight down outliers during the minimization process. Experiments show that the Leclerc influence function defined as $\rho_\eta(r) = 1+e^{-r^2/\eta^2}$ gives more stable results even if no significant differences are noticeable with other M-estimators (e.g. Tukey Bi-weighted or German-McClure). On each frame, variance of pseudo-residuals is estimated using a robust least trimmed square estimator [10]; the maximum value is selected to set σ^2_{LTS}. The parameter λ_1 is a constant set to 4.

Parameters are initialized as follow : C_{S_0}, and A_{S_0} are respectively set to the average and the range of the set $\left\{\frac{I(x)(k)}{G_{\gamma^-}(x-x_0^-(k))}\right\}_{k\in[1,K^-],x\in W(x_0^-)(k)}$ and $\Phi_{\tau_0} = \Phi_{M_0} - \Phi_E + \arctan(\omega_E\tau_{EGFP})$ with τ_{EGFP} set to the fluophore lifetime measured without FRET (e.g. 2.5 nanoseconds for the EGFP presents in our experimental samples).

Step 2: Robust tracking

In this step, $x_0(k)$ is estimated for each frame $I(k), k \in [1, K]$ given θ_0^-. Tracking is performed frame-by-frame using the same robust error function as:

$$(\hat{x}_0(k), \hat{\gamma}) = \underset{(x_0(k),\gamma)}{\operatorname{argmin}} \sum_{x\in W(x_0(k))} \rho_{\eta_2}\left(I(k)(x) - S_{\theta_0^-}(k)G_\gamma(x - x_0(k))\right). \quad (9)$$

As previously, we have chosen the Leclerc error function. The scale parameter $\eta_2 = \lambda_2\sigma_{res}(k)$ is defined for each frame as [10]:

$$\sigma_{res}(k) = 1.4826 \underset{i\in[1,|W(\hat{x}_0(k))|]}{\operatorname{median}} |r_i - \underset{i\in[1,|W(\hat{x}_0(k))|]}{\operatorname{median}} |r_i|| \quad (10)$$

where $\{r_i\}_{i\in[1,|W(x_0(k)|]}$ is the set of residuals of estimation introduced in (9) when using the L^2-norm as influence function which is equivalent to a least mean square estimation of $(x_0(k), \gamma)$. The parameter λ_2 is a constant set to 4. Initialization is performed with $\gamma = \gamma^-$ and $x_0(k) = \hat{x}_0(k-1)$ ($x_0(0)$ is determined by spot detection).

Step 3: lifetime estimation

In this step θ_0 is estimated by taking advantage of the estimates $\hat{x}_0(k)$ for $k \in [1, K]$. As the measure must be as precise as possible, we do not neglect the influence of the background. Background estimation relies on cytoplasmic auto-fluorescence described by $S_{\theta_b}(k)(x)$ in (4). Therefore we estimate $\theta_b(x)$ for $x \in \bigcup_{k\in[1,K]} W(\hat{x}_0(k))$ and furthermore subtract $S_{\theta_b}(k)(x)$ from each frame $I(k)$. Similarly to [11] we use an asymmetric M-estimator to discriminate background over vesicles. This modeling approach does not handle still particles; if a vesicle does not move, there is no way to interpolate the underlying background. Hence we consider the neighboring pixels yielding to:

$$\hat{\theta}_b(x) = \underset{\theta_b}{\operatorname{argmin}} \sum_{w\in W(x)} \sum_{k\in[1,K]} \rho_{\eta_3}\left(I(k)(w) - S_{\theta_b}(k)(x)\right), \quad (11)$$

for $x \in \bigcup_{k\in[1,K]} W(\hat{x}_0(k))$, where $W(x)$ is a 7×7 square window centered at x. As in [11], we have chosen an asymmetric Leclerc error function with $\eta_3 = \lambda_3\sigma_{res}(k)$, λ_3 is set to 3 for positive residuals and 9 for negative residuals. Over-weighting the negative residual disadvantage the pixel belonging to a spot, as the results θ_b describe the intensity of the background (see Fig. 3).

After background subtraction, θ_0 is estimated as in Step 1 from the total number of K frames (instead of K^-). It comes the parameter Φ_{τ_0} and $\tau_0 = \frac{\tan(\Phi_{\tau_0} - \Phi_{M_0} + \Phi_E)}{\omega_E}$ (see eq. (5).

4. RESULTS AND DISCUSSION

This section presents our experimental results conducted on both synthetic and real samples.

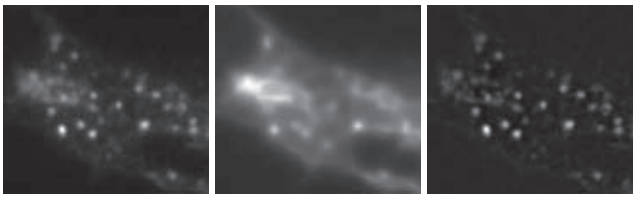
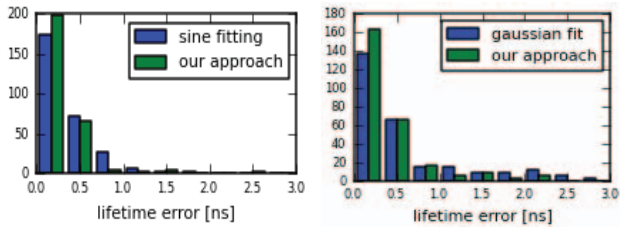


Fig. 3. Background estimation on an experimental sample.



(a) Lifetime estimation method (b) Tracking method

Fig. 4. Comparing vesicle lifetime histograms from simulations.

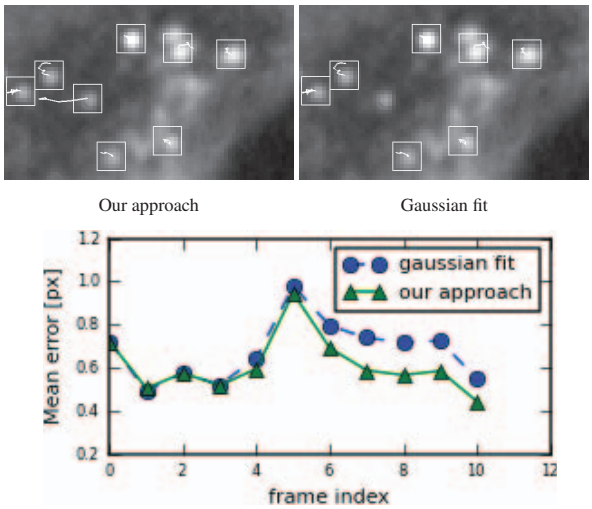


Fig. 5. Comparing the average track error of 30 vesicles in a real image sequence.

Synthetic data Our simulations are based on our intensity model. Background is simulated with a real vesicle-less sample and cytoplasmic fluorescence is simulated with constant parameter θ_b on the background. Vesicle intensities follow (7) and movement is limited to a two pixel range. A Poisson-Gaussian noise is then applied to alter measurements. Figure 4(a) compares lifetime estimation method on tracked vesicles while Fig. 4(b) compares our tracker with a basic Gaussian fitting coupled with same robust lifetime estimation scheme(Section 3.2).

Real samples FLIM measurement were conducted on living cells using a confocal microscope with spinning disk setup (UMR 144 CNRS-PICT Institut Curie). Uncontrolled vesicle interactions on experimental samples makes the generation of ground truth of lifetime impossible. Nevertheless we compared the accuracy of tracking results. Tracks have been manually measured using MJtrack software [7]. Figure 4 shows that tracking performance is lower on the darkest frames. Additional investigations led us to focus more on the noise induced by instrumentation to tackle this issue in future works. Figure 2 shows an example of lifetime map reconstruction, estimated lifetime value is imposed as a patch of radius $\hat{\gamma}$ on the vesicle position $\hat{x}_0(0)$.

5. CONCLUSION

Our method allows to recover lifetime of moving vesicles in an efficient and fast way in frequency-domain FLIM imaging. This study shows the importance of taking the intensity model into account while tracking vesicles. Other trackers such as linking method will be quantitatively compared to assess the differences in performance of our procedure which is much less demanding in the spot detection area.

6. REFERENCES

[1] M.A. Hink, T. Bisseling, and A.J.W.G. Visser, "Imaging protein-protein interactions in living cells," *Plant molecular biology*, vol. 50, no. 6, pp. 871–883, 2002.

[2] K. Suhling, P.M.W. French, and D. Phillips, "Time-resolved fluorescence microscopy," *Photochemical & Photobiological Sciences*, vol. 4, no. 1, pp. 13–22, 2005.

[3] BQ Spring and RM Clegg, "Image analysis for denoising full-field frequency-domain fluorescence lifetime images," *Journal of Microscopy*, vol. 235, no. 2, pp. 221–237, 2009.

[4] J.R. Lakowicz and B.R. Masters, "Principles of fluorescence spectroscopy," *Journal of Biomedical Optics*, vol. 13, pp. 029901, 2008.

[5] E. Meijering, I. Smal, and G. Danuser, "Tracking in molecular bioimaging," *IEEE Signal Processing Magazine*, vol. 23, no. 3, pp. 46–53, 2006.

[6] N. Chenouard, A. Dufour, and J.C. Olivo-Marin, "Tracking algorithms chase down pathogens," *Biotechnology Journal*, vol. 4, no. 6, pp. 838–845, 2009.

[7] I. Smal, M. Loog, W. Niessen, and E. Meijering, "Quantitative comparison of spot detection methods in fluorescence microscopy," *IEEE Transactions on Medical Imaging*, vol. 29, no. 2, pp. 282–301, 2010.

[8] S. Bonneau, L. Cohen, and M. Dahan, "A multiple target approach for single quantum dot tracking," in *Biomedical Imaging: Nano to Macro, 2004. IEEE International Symposium on*. IEEE, 2004, pp. 664–667.

[9] C.M. Anderson, G.N. Georgiou, IE Morrison, GV Stevenson, and R.J. Cherry, "Tracking of cell surface receptors by fluorescence digital imaging microscopy using a charge-coupled device camera.," *Journal of Cell Science*, vol. 101, no. 2, pp. 415, 1992.

[10] P.J. Rousseeuw, A.M. Leroy, and J. Wiley, *Robust regression and outlier detection*, vol. 3, Wiley Online Library, 1987.

[11] J. Boulanger, C. Kervrann, and P. Bouthemy, "Estimation of dynamic background for fluorescence video-microscopy," in *Image Processing, 2006 IEEE International Conference on*. IEEE, 2006, pp. 2509–2512.